



Original article

Land use and land cover change impact on forest carbon storage in Raktamala community forest, Nepal

Satish Kumar Singh^{a*}, Menuka Maharjan^{a,b}, Saroj Kumar Das^c

^a School of Forestry and Natural Resource Management, Institute of Forestry, Tribhuvan University, Kathmandu, Nepal

^b Institute of Forestry, Hetauda Campus, Tribhuvan University, Hetauda, Nepal

^c Institute of Forestry, Pokhara Campus, Tribhuvan University, Nepal

ARTICLE INFO

Keywords:

Carbon stock
Business-as-usual scenario
Community forest
Remote sensing

ABSTRACT

The Chure mountain range of Nepal is witnessing rapid changes in land use and land cover (LULC) due to increasing anthropogenic pressures, with significant implications for forest carbon storage. This study assesses the impact of the LULC changes on forest carbon in Raktamala Community Forest (CF), Saptari, using remote sensing, Geographic Information System and field-based methods. A total of 56 circular plots, with radii of 12.61 m for trees, 2.82 m for saplings and 1.87 m for soil, were established in the field. Tree diameter at breast height and height were measured, and carbon was estimated for aboveground biomass, belowground roots, saplings and soil. The results indicated a decline in forest cover from 54% in 2000 to 52% in 2022. The average carbon stock in 2022 was $156.60 \pm 13.42 \text{ t ha}^{-1}$. Under a business-as-usual scenario, the estimated total forest carbon and CO₂ equivalents for 2000 and 2010 were 28,537.52 t (104,447.3 t CO₂) and 27,962.5 t (102,342.7 t CO₂) respectively. These findings support the development of the Reducing Emissions from Deforestation and Forest Degradation baselines and sustainable forest management.

INTRODUCTION

Land use and land cover (LULC) change is a major global environmental challenge that influences the ecosystem structure, biodiversity and the terrestrial carbon (C) cycle. While land cover describes the physical features of the earth's surface, land use reflects the ways humans utilize these resources (Dimyati et al., 1996). Changes in LULC alter soil processes, hydrological systems and atmospheric conditions, thereby shaping whether ecosystems function as carbon sinks or sources (Foley et al., 2005). Forests are particularly important, storing large proportions of terrestrial carbon, with recent assessments estimating approximately 650 billion tonnes stored globally (FAO, 2020; Pan et al., 2011). As deforestation and forest degradation contribute roughly 10–12% of annual anthropogenic CO₂

emissions (IPCC, 2021), monitoring the LULC change remains essential for climate mitigation efforts, including Intergovernmental Panel on Climate Change-aligned national greenhouse gas reporting and Reducing Emissions from Deforestation and Forest Degradation (REDD+) initiatives.

Recent advancements in remote sensing and geographic information systems have improved the accuracy of land cover mapping and biomass estimation (Chuvieco et al., 2019). These tools are increasingly used across South Asia, where population growth, agricultural expansion and resource extraction continue to reshape landscapes (Lamichhane et al., 2021). In Nepal, forests cover approximately 43.38% of the country's land area, with Other Wooded Land contributing an additional 2.70% (FRTC, 2024). However, the Chure mountain range, geologically young and erosion-prone, remains highly susceptible

* Corresponding author:

E-mail address: singhsatish7736@gmail.com

doi: <https://doi.org/10.3126/forestry.v22i1.84201>

Received: 8 Sept 2025; Revised in received form: 8 Dec 2025 Accepted: 10 Dec 2025

© The Authors. Published by Institute of Forestry, Tribhuvan University. This is an open access article under the CC BY license (<http://creativecommons.org/licenses/by/4.0/>).

to degradation (Pokhrel, 2013; Thapa et al., 2023). Human pressures, including overgrazing, sand and gravel extraction, unplanned cultivation, road construction and forest fires, have accelerated soil erosion and reduced forest carbon stocks (Dudhaura et al., 2015; Lamichhane et al., 2021). Strengthening spatially explicit assessments in this region is crucial for guiding interventions under national and provincial conservation programmes, including the President Chure-Terai Madhesh Conservation Project.

Although several studies in Nepal have examined land cover dynamics using satellite imagery (eg Shrestha et al., 2021) or quantified forest carbon stocks through field-based inventories (eg Gautam et al., 2022), very few have integrated both approaches to understand how spatiotemporal LULC change influences forest carbon dynamics. This gap is particularly notable in community forests (CFs), which represent one of Nepal's most significant forest management systems (DFRS, 2015). To address this research gap, the present study analyses LULC change and associated carbon storage dynamics over a 22-year period (2000–2022) in Raktamala Community Forest (CF) in Nepal's Chure region. By combining multi-temporal satellite imagery with field-based biomass data, this study aims to generate evidence that strengthens community-based

forest management, informs REDD+ readiness, and supports policy interventions in carbon-sensitive and erosion-prone landscapes.

MATERIALS AND METHODS

Study area

Raktamala CF (latitude: 26° 44'31.84" N and longitude: 86° 55' 12.33" E) lies in Saptakoshi Municipality in Saptari District, Nepal, and covers 374.42 ha of forest area (Figure 2). The CF is situated in the northern part of the district within the Chure mountains, where the soil contains small rock pebbles, stones and sand (DFO Saptari, 2019). The topography of the study area shows little variation, with elevations ranging between 115 m and 300 m above mean sea level (DFO Saptari, 2019). The highest temperatures, between 30 °C and 46 °C, occur from February to July, while the average winter temperature ranges from 15 °C to 18 °C, with a minimum of 7 °C (DFO Saptari, 2019). The dominant species in the region, based on the terrain, include *Shorea robusta*, *Syzygium cumini*, *Lagerstroemia parviflora*, *Mallotus philippinensis* and *Anogeissus latifolia*.

Raktamala CF was selected for this study because it is representative of the Chure region's forest ecosystem,

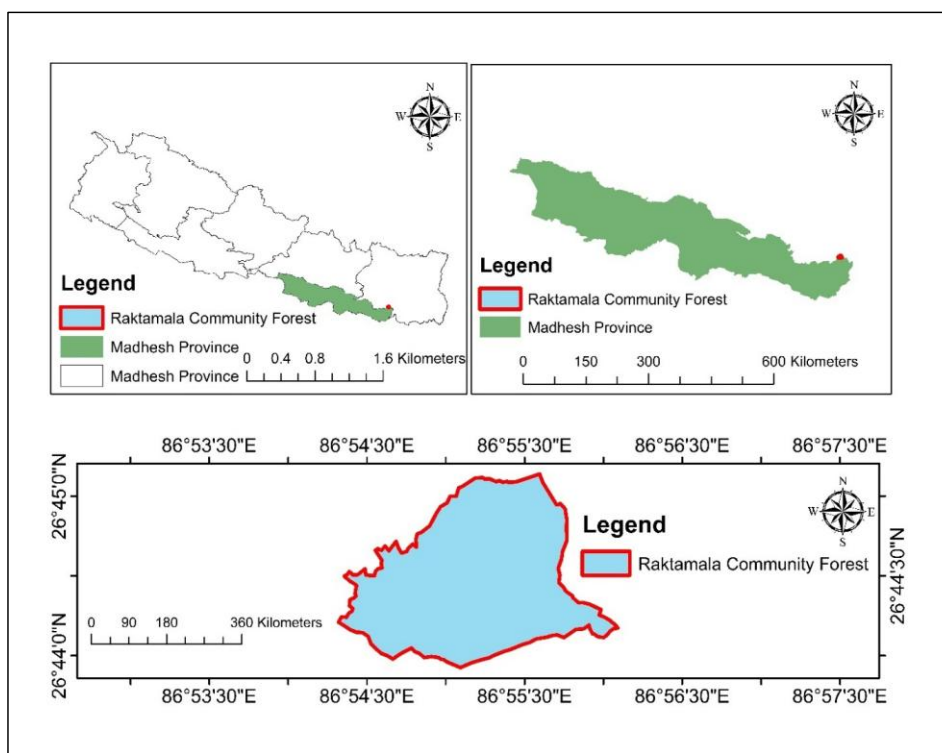


Figure 1: Location map of the study area

is easily accessible for field data collection and has an active community management programme that facilitates participatory research and validation of field observations.

Satellite data

Landsat 7 and Landsat 8 satellite imagery for 2000, 2010 and 2022 was used to analyse the LULC changes (Figure 2). Images were sourced from USGS (<https://earthexplorer.usgs.gov/>), selecting data with < 20% cloud cover, and all images were from Landsat Collection 1 Level 1, which provides geometrically and radiometrically calibrated data.

Table 1: Specifications of the Landsat data

WRS (Path/Row)	Scene ID	Sensor	Spatial Resolution	Acquired Date
Path=140	LE71400	Enhanced Thematic Mapper (ETM)	30*30	2000/03/04
Row= 41	41200006			
	4SGS00			
Path=140	LE71400	Enhanced Thematic Mapper (ETM)	30*30	2010/02/28
Row= 41	41201005			
	9SGS00			
Path=140	LC81400	Operational Land Imager and Thermal Infrared Sensor (OLI_TIRS)	30*30	2022/02/21
Row= 41	41202205			
	2LGN00			

Sampling design and sample plot layout

Field data for vegetation and carbon measurements were collected during the third week of March 2023 over a period of seven days, during the dry season, to ensure comparability with the satellite imagery acquisition period. Systematic random sampling stratified the forest into regeneration, poles and trees (Cochran, 1977; Krebs, 1999). Circular plots were used to minimize edge effects and adapt to sloping terrain (Boon, 1966). The sampling intensity was 1%, with 53 final sample plots established using ArcGIS 10.5. Plots of 500 m² (radius 12.61 m) were used for trees (≥ 5 cm DBH), nested plots of 25 m² (radius 2.82 m) for saplings (1–5 cm DBH) and 1 m² plots for seedlings (< 1 cm DBH). Soil samples were collected from 1.87 m radius subplots.

Aboveground tree biomass (AGTB) and belowground biomass (BGB)

Tree DBH and height were measured using a diameter tape and a rangefinder. Biomass was calculated using allometric equations (Chave et al., 2005). Sapling biomass was estimated from national allometric tables (Tamrakar, 2000). Deadwood, litter and leaves were excluded due to local collection practices (Adhikari et al., 2004). Root biomass was estimated using a root: shoot ratio of 0.125, as recommended for tropical forests (IPCC, 2006).

Soil

Soil samples were collected from a depth of 0–30 cm at each plot, using a metal corer. Sampling was conducted at a single depth to maintain consistency in the soil organic carbon (SOC) analysis. At each plot, a single soil core was collected, as composite sampling was not applied in this study. A total of 53 soil samples

were collected from circular subplots, with a radius of 1.87 m established across the study area. The samples were placed in labelled sample bags (Gautam, 2020) and transported to the laboratory. The SOC of soil samples was analysed using the Walkley-Black method (Walkley & Black, 1934) in the laboratory. Bulk density was estimated by oven-drying the samples at 105 °C (De Vos et al., 2007).

Data analysis

Image processing and classification

Atmospheric correction was performed using the USGS Surface Reflectance products for both Landsat 7 and Landsat 8 imagery. To minimize radiometric differences between Landsat 7 and Landsat 8 images, histogram matching was applied over invariant target areas. For LULC classification, a total of 140 training samples (20 samples per class for 7 classes) were used, and 30% of these training samples were randomly selected for validation. The classification utilized the Blue, Green, Red, NIR, SWIR1 and SWIR2 bands, along with NDVI, to improve vegetation and land cover discrimination. A supervised classification approach using the Maximum Likelihood Classifier was applied, utilizing training samples from six LULC categories: Waterbody, Built-up Area, Forest, Riverbed, Grassland, Cropland and Other Wooded Land (OWL) (Sisodia et al., 2014).

LULC Change Detection and Accuracy Assessment

Post-classification comparison was used to detect the LULC changes between 2000 and 2022, and the total LULC change was calculated using equation (1). Kappa coefficient values were interpreted using standard thresholds, where < 0.20 indicates poor agreement, 0.21–0.40 fair, 0.41–0.60 moderate, 0.61–0.80 substantial and > 0.80 represents almost perfect agreement. Kappa statistic ($\hat{\kappa}$) was computed (equation 2) according to Salih (1983).

$$\begin{aligned} \text{Percentage of LULC} \\ = \frac{\text{Area of final year} - \text{Area of the initial year}}{\text{Area of the initial year}} \\ * 100 \text{ eqn (1)} \\ \hat{\kappa} = \frac{N \sum_{i=1}^r x_{ii} - \sum_{i=1}^r (x_{i+} \cdot x_{+i})}{N^2 - \sum_{i=1}^r (x_{i+} \cdot x_{+i})} \text{ eqn (2)} \end{aligned}$$

where, r = number of rows in the error matrix, x_{ii} = number of observations in row i and column i (on the major diagonal), x_{+} = total of observations in row i (shown as marginal total to the right of the matrix), x_{+i} = total of observations in column i (shown as marginal total at bottom of the matrix), N = total number of observations included in the matrix

Biomass and carbon estimation

Above-ground tree biomass (AGTB): Estimated using Chave et al. (2005) (equation 3)

$$\text{AGTB} = 0.0509 \times \rho D^2 H \text{ eqn (3)}$$

Where, AGTB = aboveground tree biomass (kg), ρ = dry wood density ($\frac{\text{g}}{\text{cm}^3}$), D = tree diameter at breast height (cm), H = tree height (m)

Above-ground sapling biomass (AGSB): Derived from DFRS and TISC allometric tables (Tamrakar, 2000).

$$\ln(\text{AGSB}) = a + b \ln(D) \text{ eqn (4)}$$

Where, \ln = Natural log; (dimensionless), AGSB = Aboveground sapling biomass; (kg), a = Intercept of allometric relationship for saplings; (dimensionless), b = Slope allometric relationship for saplings; (dimensionless), D = Over bark diameter measured at breast height; (cm)

Below-ground biomass (BGB): Estimated using IPCC's (2006) root-to-shoot ratio of 0.125.

Conversion to carbon: Biomass converted to carbon using a factor of 0.47 (Andreae & Merlet, 2001).

SOC: Estimated via the Walkley–Black method (1958), incorporating bulk density and carbon concentration (Equation 5).

$\text{SOC} = \text{Organic carbon content percentage}$

$$* \text{soil bulk density} \left(\frac{\text{g}}{\text{cm}^3} \right)$$

$$* \text{thickness of soil horizon eqn(5)}$$

Where, SOC = Soil Organic Carbon stock per unit area (t h^{-1}), % Carbon = Carbon concentration, ρ = soil bulk density (g/cm^3), d = total depth (cm)

Total Carbon Calculation

The total carbon stock was calculated using (Equation 6).

$$C(\text{TB}) = C(\text{AGTB}) + C(\text{AGSB}) + C(\text{BB}) + \text{SOC} \text{ eqn(6)}$$

Where, $C(\text{TB})$ = Total Carbon Stock Biomass (t C h^{-1}), $C(\text{AGTB})$ = Carbon in aboveground tree biomass (t C h^{-1}), $C(\text{AGSB})$ = Carbon in aboveground sapling biomass (t C h^{-1}), $C(\text{BB})$ = Carbon in belowground biomass (t C h^{-1}), SOC = Soil Organic Carbon (t C h^{-1}).

Uncertainty Estimation

Uncertainty was expressed as mean \pm SD. Standard measurement errors ($\text{DBH} \pm 0.5 \text{ cm}$, height $\pm 0.2 \text{ m}$, wood density $\pm 10\%$) were used and propagated through allometric equations. Carbon component uncertainties were assumed as $\pm 10\%$ (AGTC, BGRC), $\pm 20\%$ (AGSC) and $\pm 15\%$ (SOC), with total carbon uncertainty derived by combining component variances.

Forest Carbon Estimation and LULC Impact
Due to the absence of field data for 2000 and 2010, forest carbon stocks for these years were estimated under a business-as-usual scenario based on the 2022 field-measured values and corresponding LULC proportions (Equations 7, 8, 9 and 10).

Carbon stock of 2000

Carbon stock of 2000 = Carbon stock t h^{-1} of 2022 * forest area of 2000 eqn(7)

CO_2 equivalent of 2000 = Carbon stock of 2000 * 44/12 (IPCC, 2006) eqn(8)

Carbon Stock of 2010

Carbon stock of 2010 = Carbon stock t h^{-1} of 2022 * forest area of 2010 eqn(9)

CO_2 equivalent of 2010 = Carbon stock of 2010 * 44/12 (IPCC, 2006) eqn(10)

To assess the impact of the LULC changes on forest carbon stock, this study applied equations 11 and 12 to estimate carbon stock changes for 2000, 2010 and 2022. This method, based on Houghton (2003) and Brown & Gaston (1995), enables direct comparison of carbon stocks across time, and is widely used in carbon budget assessments (Harris et al., 2012; Pan et al., 2011).

$$\Delta C_{2000-2022} = C_{2022} - C_{2000} \text{ eqn (11)}$$

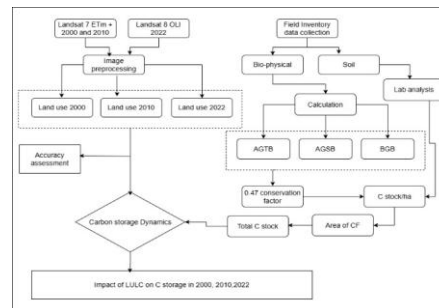
$$\Delta C_{2010-2022} = C_{2022} - C_{2010} \text{ eqn (12)}$$

Whereas, C_{2022} , C_{2000} , C_{2010} represent the total carbon stock in the forest for the years 2022, 2000 and 2010 respectively.

$\Delta C_{2000-2022}$ represents the total change in forest carbon stock between 2000 and 2022.

$\Delta C_{2010-2022}$ represents the total change in forest carbon stock between 2010 and 2022.

The overall methodological flow chart outlines the sequential steps undertaken, including satellite image acquisition, LULC classification, field data collection, carbon stock estimation and change analysis across different periods (2000, 2010 and 2022) (Figure 2).



*AGTB: Above Ground Tree Biomass, AGSB: Above Ground Sapling Biomass, BGB: Below Ground Biomass

Figure 2: Methodological flow chart

RESULTS

Analysis of land use and land cover classes for 2000, 2010 and 2022

The LULC maps for 2000, 2010 and 2022 demonstrate the spatial dynamics of land cover changes over the study period within the boundary of Raktamala CF (Figure 3). In 2000, LULC was dominated by forests (54.25%), followed by riverbed (18.55%), grassland (10.97%), cropland (9.02%), waterbody (4.94%), OWL (1.33%), and built-up area (0.94%) (Table 2). By 2010, the forest remained the major land cover type (53.15%), with riverbed (12.23%), grassland (12.23%), cropland (9.55%), waterbody (4.32%), built-up area (1.19%), and OWL (1.12%) showing slight changes (Table 2). In 2022, forest cover continued to decline (51.60%), while riverbed (16.52%), grassland (11.86%), cropland (8.40%),

waterbody (6.81%), OWL (3.05%), and built-up area (1.77%) showed varying trends.

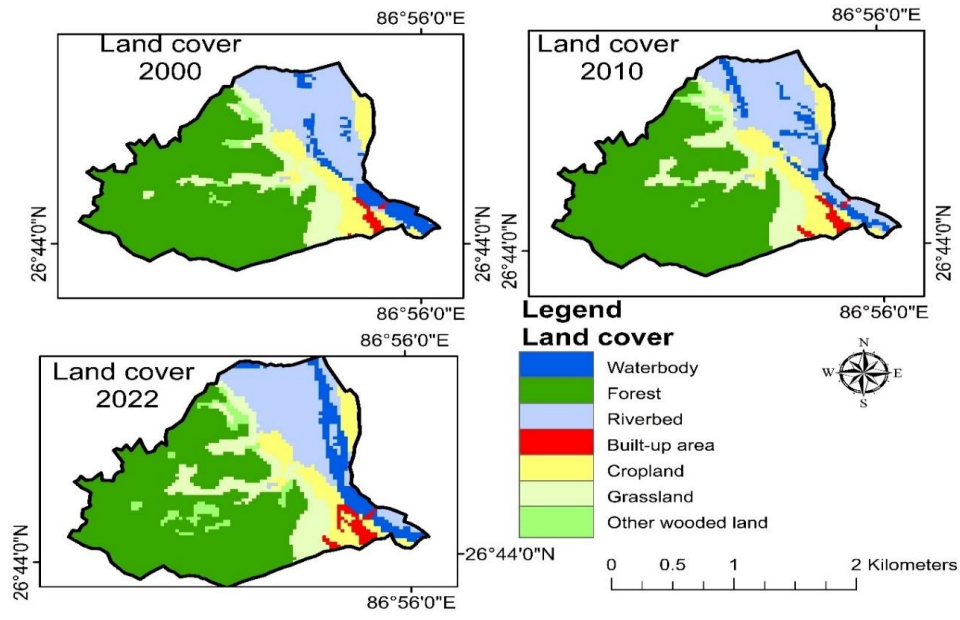


Figure 3: LULC map of 2000, 2010, and 2022

Table 2: Area statistics of different LULC classes

LULC type	2000		2010		2022	
	Area (ha)	Proportion (%)	Area (ha)	Proportion (%)	Area (ha)	Proportion (%)
Waterbody	18.43	4.94%	16.12	4.32%	25.43	6.81%
Forest	202.48	54.25%	198.40	53.15%	192.67	51.60%
Riverbed	69.25	18.55%	68.82	18.44%	61.68	16.52%
Built-up area	3.50	0.94%	4.46	1.19%	6.62	1.77%
Cropland	33.65	9.02%	35.64	9.55%	31.36	8.40%
Grassland	40.95	10.97%	45.66	12.23%	44.28	11.86%
OWL	4.98	1.33%	4.19	1.12%	11.38	3.05%
Total	373.24	100.00%	373.24	100.00%	373.24	100.00%

Accuracy Assessment

For accuracy assessment, we generated reference points through visual interpretation of the high-resolution Google Earth imagery corresponding to the same time period of the Landsat scenes. These reference samples were used to prepare the confusion matrix and compute overall accuracy, user's accuracy and producer's accuracy. The classification accuracies of LULC for 2000, 2010 and 2022 were evaluated, yielding kappa coefficients of 0.91, 0.90 and 0.86 respectively, with overall accuracies of 90%, 90% and 88%.

Table 3: Accuracy assessment of LULC classification for 2000, 2010 and 2022, including producer's accuracy, user's accuracy, overall classification accuracy and Kappa statistics for each LULC class

LULC Class	2000		2010		2022	
	PA	UA	PA	UA	PA	UA
Waterbody	0.94	0.90	0.94	0.85	0.89	0.85
Forest	1.00	0.95	0.86	0.95	0.94	0.85
Riverbed	0.86	0.95	0.82	0.85	0.80	0.85
Built-up area	1.00	0.95	1.00	0.90	0.94	0.90
Cropland	0.90	0.90	0.90	0.90	0.90	0.90
Grassland	0.85	0.90	1.00	0.90	0.81	0.90
OWL	0.95	0.95	0.90	0.95	0.90	0.95
Year	2000		2010		2022	
Overall Classification Accuracy	90.00%		90.00%		88.00%	
Overall, Kappa Statistics	0.91		0.90		0.86	

LULC status analysis

The LULC classes that had consistently increased were built up, while forest and riverbed areas were constantly decreased. Forest (54–52%) and riverbed (19–17%) covers have decreased between 2000 and 2022. The built-up area has increased from 0.94% to 1.77% between 2000 and 2022. Cropland and grassland areas experienced fluctuations over the years (2000–2022). Between 2000 and 2022, the waterbody and OWL expanded by 1.87% and 1.72% respectively.

Land use and land cover change transition matrix from 2000 to 2022

The Sankey diagram illustrates the LULC transitions from 2000 to 2022, showing directional changes in forest, grassland, cropland and riverbed (Figure 4). The largest transition occurred from riverbed to waterbody, accounting for 15.96 ha (Table 4). Forest land experienced a conversion of 7.65 ha into built-up areas, while cropland underwent a notable transition of 2.60 ha into built-up areas. Grassland transitioned into forest land, covering 3.15 ha. Moreover, a greater extent of cropland (3.33 ha) transitioned to built-up areas compared to forest land.

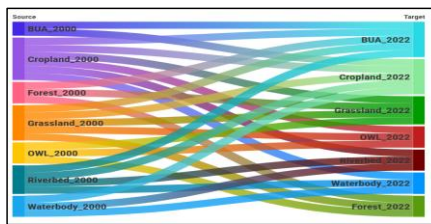


Figure 4: LULC change dynamics from 2000 to 2022 depicted in a Sankey diagram

Table 4: Transition matrix from 2000 to 2022

LULC_2000 (ha)	LULC_2022 (ha)							
	Built-up area	Cropland	Forest	Grassland	Other wooded land	Riverbed	Waterbody	Grand Total
Built-up area	3.33	0.08	0	0	0	0	0.07	3.48
Cropland	2.60	30.03	0	0.10	0.22	0.13	0.54	33.62
Forest	7.65	0	188.42	6.15	0	0	0	202.22
Grassland	0.40	0.19	3.15	34.60	2.54	0	0	40.88
OWL	0	0	0.58	1.94	2.47	0	0	4.99
Riverbed	0.23	0.43		0	0	52.33	15.96	68.95
Waterbody	0	0.63	0	0	0	9.04	8.73	18.4
Grand Total	14.21	31.36	192.15	42.79	5.23	61.5	25.3	374.52

Biomass and carbon stock of Raktamala CF

Biomass stock

The estimated tree biomass in Raktamala CF was $175.14 \pm 18.76 \text{ t ha}^{-1}$, representing the largest share of the total biomass (Figure 5). In contrast, sapling biomass was much smaller, contributing only $0.36 \pm 0.08 \text{ t ha}^{-1}$. The BGB, including roots and other subterranean components, was $21.93 \pm 2.19 \text{ t ha}^{-1}$. Consequently, the total biomass, comprising both AGB and BGB, amounted to $197.43 \pm 19.92 \text{ t ha}^{-1}$.

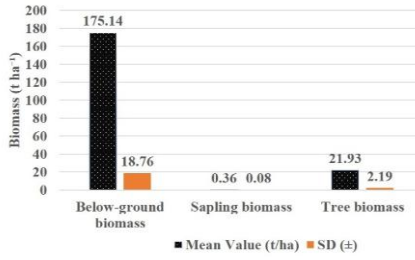


Figure 5: Biomass distribution in Raktamala CF

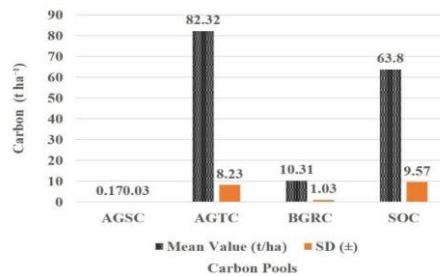
Carbon stock

The carbon stock in Raktamala CF was quantified for various components (Figure 6). The aboveground tree carbon (AGTC) stock was $82.32 \pm 8.23 \text{ t ha}^{-1}$, indicating a major contribution to the forest's total carbon pool. The aboveground sapling carbon (AGSC) stock, although smaller, was $0.17 \pm 0.03 \text{ t ha}^{-1}$. The belowground root carbon (BGRC) stock accounted for $10.31 \pm 1.03 \text{ t ha}^{-1}$. The SOC stock was $63.80 \pm 9.57 \text{ t ha}^{-1}$, representing the carbon stored in the top 30 cm of forest soil, based on laboratory analysis. Collectively, the total ecosystem carbon stock of the forest, combining all components, was $156.60 \pm 13.42 \text{ t ha}^{-1}$.

Impact of LULC Change on Forest Carbon

Forest Area over Time

The forest area has steadily decreased from 202.48 ha in 2000 to 198.40 ha in 2010 and further to 192.67 ha in 2022 (Table 2). This signifies a net loss of about 10 ha between 2000 and 2022.



Note: AGSC: Aboveground Sapling Carbon, AGTC: Aboveground Tree Carbon, BGRC: Belowground Root Carbon, SOC: Soil Organic Carbon

Figure 6: Total carbon stock in Raktamala CF

Commented [at1]: Check this section with Figure 6 arrangement

Total Carbon Storage

The reduction across all scenarios indicates a general decline in carbon sequestration over time (2000–2022). In the business-as-usual scenario, total carbon storage decreased from 31,708.36 t in 2000 to 30,172.12 t in 2022, representing a 5% reduction (Table 5). Similarly, the scenario assuming a 5% reduction in carbon shows a decrease from 30,122.94 t in 2000 to 28,663.51 t in 2022. In the scenario with a 10% reduction, total carbon dropped from 28,537.52 t in 2000 to 27,154.91 t in 2022. The reduction across all scenarios indicates a general decline in carbon sequestration over time (Table 5).

CO₂ Equivalent of Forest Carbon Stock

The trends demonstrate a consistent decline in total CO₂ equivalent values derived from forest carbon stock estimates under a business-as-usual scenario over twenty-two years (2000–2022) (Table 5). This indicates a gradual reduction in the forest's carbon storage potential rather than a decrease in actual CO₂ emissions. Under the business-as-usual scenario, the CO₂ equivalent value decreased from 116,264.01 t in 2000 to 110,631.11 t in 2022. In the 5% reduction scenario, CO₂ equivalents declined from 110,450.78 t to 105,099.55 t over the same period. Similarly, under the 10% reduction scenario, CO₂ equivalent values dropped from 104,447.30 t in 2000 to 99,386.96 t in 2022. These results reflect a steady loss in the forest's capacity to sequester and store CO₂ over time.

Year	Forest Area (ha)	Business-as-usual Total carbon (t)	Business-as-usual Total CO ₂ equivalent (t)	Total carbon (t)	Total CO ₂ equivalent (t)	Total carbon (t)	Total CO ₂ equivalent (t)
				Business-as-usual scenario		Assuming 5% less carbon	
2000	202.48	31708.36	116264.01	30122.94	110450.78	28537.52	104447.3
2010	198.40	31069.44	113921.28	29515.96	108225.21	27962.5	102342.7
2022	192.67	30172.12	110631.11	28663.51	105099.55	27154.91	99386.96

DISCUSSION

Land use land cover change dynamics

Between 2000 and 2022, Raktamala CF experienced a 4.84% decline in forest cover (Table 2), primarily due to its conversion into built-up areas and grasslands, mirroring regional forest loss patterns in Nepal's Chure mountains (FAO, 2012; DFRS, 2015). The decline in forest cover is primarily driven by local pressures such as intensive grazing, sand and gravel mining, and recurring forest fires, which suppress natural regeneration, accelerate erosion and reduce biomass (Acharya *et al.*, 2019; Joshi *et al.*, 2024). These localized disturbances are key drivers of forest degradation in Raktamala CF and provide an essential context before broader regional and global comparisons. Such deforestation reduces carbon storage and contributes to increased CO₂ emissions (Houghton, 2003), highlighting the need for sustainable land use (Lambin & Meyfroidt, 2011).

In Raktamala CF, built-up areas increased by 89.14% (Table 4), with 7.65 ha of forest and 2.60 ha of cropland converted into settlements, reflecting rising development pressures. This transformation, including small-scale structures, like huts and internal paths, led to habitat fragmentation and forest degradation. Similar unplanned urbanization trends across Nepal have intensified ecological stress (Pantha *et al.*, 2024; Thapa & Murayama, 2011), reinforcing calls for environmentally-sound urban planning.

Cropland decreased by 6.81%, with agricultural displacement promoting forest encroachment—consistent with global interactions among urban expansion, agriculture and forests (Lamichhane *et al.*, 2021). Such transitions often lead to biodiversity loss and reductions in ecosystem services, such as carbon storage (Geist & Lambin, 2001; Houghton, 2012).

Hydrological changes and grassland expansion in Raktamala CF reflect combined land-use pressures, driven by deforestation, erosion and human disturbances. Riverbeds and waterbodies increased by 61.5 ha and 18.4 ha respectively (Table 4), mainly due to forest loss, sediment deposition and sand mining (Acharya & Paudel, 2022; Mishra *et al.*, 2020). Grasslands similarly expanded through conversions of forest (6.15 ha) and cropland (0.10 ha), indicating reduced regeneration and intensified grazing pressure (FAO, 2020; Chaudhary *et al.*, 2017). Conversions of forest and cropland into riverbeds, waterbodies and grasslands (Gautam *et al.*, 2023; Shrestha *et al.*, 2019) highlight landscape instability, declining carbon storage capacity and weakening hydrological functions. Although transitions to OWL indicate some community-based restoration efforts (Shrestha *et al.*, 2018), sustained measures, such as riparian rehabilitation, erosion control and regulated grazing, are essential to maintain ecosystem services (Lambin & Meyfroidt, 2011; Sharma & Pandey, 2022).

Transitions to OWL further suggest ongoing reforestation and community forestry initiatives. However, continued management is required to balance ecological integrity with socioeconomic needs. OWL and grassland ecosystems are vital for grazing,

biodiversity support and carbon storage. Controlled grazing, integrated land-use planning and sound community-based forest management practices are essential to maintaining long-term ecosystem resilience (Chaudhary *et al.*, 2017).

Carbon stock

The average carbon stock in Raktamala CF was 156.60 ± 13.42 t ha⁻¹ (Figure 6), slightly below the national average of 203 t ha⁻¹ for Nepal (FAO, 2012). This variation can be attributed to differences in species composition, tree size and density (Gautam, 2020). Larger trees and denser forests typically store more carbon (Brown and Gaston, 1995), and management practices, including selective logging and grazing, can influence forest carbon stocks (Lamsal *et al.*, 2023). Additionally, regional factors such as soil fertility, climate and disturbance history further contribute to carbon variability across Nepal's diverse topography (Acharya *et al.*, 2011).

The SOC stock in Raktamala CF was estimated at 63.8 ± 9.57 t ha⁻¹ (Figure 6), highlighting the critical role of forest ecosystems in carbon sequestration. This value is consistent with the SOC stocks reported in other CFs in the Chure mountains, which range from 50 to 80 t ha⁻¹ (Shrestha *et al.*, 2020). However, it is lower than the values found in the Terai and mid-hills of Nepal, where SOC stocks can exceed 100 t ha⁻¹ (Bhandari *et al.*, 2021). Several factors influence the SOC levels, including dense vegetation, climatic conditions and land-use change (Johnson *et al.*, 2019; Kumar & Singh, 2020). SOC is also affected by forest cover, with higher concentrations beneath tree-dominated areas (Edmondson *et al.*, 2014).

Impact of forest cover on forest carbon

Between 2000 and 2022, forest carbon stocks in Raktamala CF declined by 4.84% (Table 5), highlighting the impact of LULC changes on forest carbon sequestration. This decline aligns with global and regional findings on deforestation-driven carbon loss (Baccini *et al.*, 2019; Houghton, 2005; Pan *et al.*, 2011; Pugh *et al.*, 2019) and underscores the need for sustainable land management (Lambin & Meyfroidt, 2011). The 1,536.24 t carbon loss (Table 5) shows that even small-scale land conversions significantly affect ecosystem function.

Despite management actions like afforestation, fire control and sustainable harvesting, forest area and carbon stocks continued to decline. Scenario analyses further confirmed that the LULC change significantly reduces carbon sequestration potential, with even 5–10% stock losses affecting long-term carbon dynamics (Erb *et al.*, 2018; Grace *et al.*, 2014). Similar reductions due to land conversions have been documented in Sikkim, India (Sharma & Rai, 2007), and the strong link between forest cover and both aboveground and SOC is well established (Edmondson *et al.*, 2014). LULC-driven tree cover loss has long-lasting impacts on carbon storage (Woodbury *et al.*, 2006), and ongoing reductions contribute to rising atmospheric CO₂, intensifying climate change (IPCC, 2021). Biodiversity, soil stabilization, water regulation and other ecosystem services are also at risk (Haddad *et al.*, 2015; MEA, 2005). Although restoration efforts exist, their

effectiveness is limited by slow forest regeneration and persistent human pressure (Acharya et al., 2019). Studies confirm that restored forests take decades to regain significant carbon stocks (Silver et al., 2000; Bonner et al., 2013), emphasizing the need for sustained protection and community-based forest governance.

Policy implication

The LULC changes observed in Raktamala CF from 2000 to 2022 have direct implications for land management and climate mitigation policies in Nepal. Our findings support the National Land Use Policy 2019, which discourages conversion of ecologically fragile land (Government of Nepal, 2019), and align with the objectives of the Forest Policy 2019, which promotes sustainable forest management and climate change mitigation. Likewise, the Chure Conservation Strategy emphasizes restoration and strict regulation of land degradation in the Chure belt (President Chure-Tarai Madhesh Conservation Development Board 2017), while Nepal's REDD + Strategy (2018) encourages improved MRV systems to strengthen carbon accounting (Government of Nepal, 2018). Similar studies in Nepal and Asia have shown that forest loss and agricultural expansion significantly impact carbon storage (Gautam et al., 2021; Hirano et al., 2014), consistent with our results. Therefore, strengthening land use zoning, controlling the conversion of forest margins and integrating CF plans in national climate policies could help reduce carbon loss and enhance forest-based climate benefits in the Chure region.

CONCLUSION

This study shows that the LULC changes in Raktamala CF have reduced forest cover and weakened carbon storage, driven by expanding settlements, shifting cropland and increasing landscape degradation. These transitions highlight the strong link between forest loss and declining carbon sequestration potential. Even though some areas are regenerating, effective community stewardship and improved land-use decisions are still necessary to reduce future carbon loss. Overall, the findings provide important baseline insights that can guide policies that support forest conservation, promote carbon-friendly management and enhance ecosystem resilience in the Chure region.

ACKNOWLEDGEMENTS

We would like to thank the Ministry of Industry, Tourism and Forest, Madhesh Pradesh, Janakapurdham, Nepal, for funding this study. We are also grateful to the respondents and field assistants from Raktamala CF for their cooperation during data collection.

REFERENCES

Acharya, R. P., Maraseni, T. N., & Cockfield, G. (2019). Local users and other stakeholders' perceptions of the identification and prioritization of ecosystem services in fragile mountains: A case study of the Chure mountain of Nepal. *Forests*, 10(5), 1–20. <https://doi.org/10.3390/f10050421>

Acharya, R., & Paudel, S. (2022). Hydrological dynamics and land use changes in the Himalayan region. *Journal of Environmental Studies*, 15(3), 45–60

Adhikari, R., Gurung, H., & Lama, T. (2021). Ecosystem services and climate resilience in riverine landscapes. *Mountain Ecosystem Reports*, 6(1), 56–74

Andreae, M. O., & Merlet, P. (2001). Emission of trace gases and aerosols from biomass burning. *Global Biogeochemical Cycles*, 15(4), 955–966. <https://doi.org/10.1029/2000GB001382>

Baccini, A., Walker, W., Carvalho, L., Farina, M., & Houghton, R. A. (2019). Response to Comment on "Tropical forests are a net carbon source based on aboveground measurements of gain and loss." *Science*, 363(6423), 1–11. <https://doi.org/10.1126/science.aat1205>

Bhandari, S., Sharma, R., & Ghimire, M. (2021). Assessment of soil organic carbon stocks in different land use systems of the Terai region, Nepal. *Journal of Environmental Management*, 287, 112307. <https://doi.org/10.1016/j.jenvman.2021.112307>

Bonner, M. T. L., Schmidt, S., & Shoo, L. P. (2013). A meta-analytical global comparison of aboveground biomass accumulation between tropical secondary forest and monoculture plantations. *Forest Ecology and Management*, 291, 73–86. <https://doi.org/10.1016/j.foreco.2012.11.033>

Boon, T. E. (1966). A circular plot method for sampling timber in uneven-aged stands. *Forest Science*, 12(1), 58–63. <https://doi.org/10.1093/forestscience/12.1.58>

Brown, S., & Gaston, G. (1995). Use of forest inventories and geographic information systems to estimate biomass density of tropical forests: Application to tropical Africa. *Environmental Monitoring and Assessment*, 38(2–3), 157–168. <https://doi.org/10.1007/BF00546760>

Chaudhary, R. P., Upadhyay, Y., & Rimal, B. (2017). Grassland ecology and management in Nepal. *Journal of Sustainable Forestry*, 36(2), 127–145

Chave, J., Réjou-Méchain, M., Búrquez, A., Chidumayo, E., Colgan, M. S., Delitti, W. B. C., Duque, A., Eid, T., Fearnside, P. M., Goodman, R. C., Henry, M., Martínez-Yrízar, A., Mugasha, W. A., Muller-Landau, H. C., Mencuccini, M., Nelson, B. W., Ngomanda, A., Nogueira, E. M., Ortiz-Malavassi, E., ... Vieilledent, G. (2014). Improved allometric models to estimate the aboveground biomass of tropical trees. *Global Change Biology*, 20(10), 3177–3190. <https://doi.org/10.1111/gcb.12629>

Chuvieco, E., Li, J., Yang, X., & Hu, T. (2019). Advances in remote sensing of ecosystem functions and services. *Remote Sensing of Environment*, 231, 111249. <https://doi.org/10.1016/j.rse.2019.111249>

Cochran, W. G. (1977). Sampling techniques (3rd ed.). John Wiley & Sons. Retrieved December 28, 2024, from <https://www.wiley.com>

Congalton, R.G., & Green, K. (2008). Assessing the Accuracy of Remotely Sensed Data: Principles and Practices, Second Edition (2nd ed.). CRC Press. <https://doi.org/10.1201/9781420055139>

De Vos, B., Lettens, S., Muys, B., & Deckers, J. A. (2007). Walkley-Black analysis of forest soil organic carbon: Recovery, limitations, and uncertainty. *Soil Use and Management*, 23(3), 221–229. <https://doi.org/10.1111/j.1475-2743.2007.00084.x>

Department of Forest Research and Survey. (2015). State of Nepal's forests: Forest resource assessment (FRA) Nepal. DFRS, Kathmandu, Nepal. https://frtc.gov.np/downloads/StateofNepalsForestsDFRS_1457599484-1729667336.pdf

Dimyati, M., Mizuno, K., Kobayashi, S., & Kitamura, T. (1996). An analysis of land use/cover change using the combination of MSS Landsat and land use map—a case study in Yogyakarta, Indonesia. *International Journal of Remote Sensing*, 17(5), 931–944. <https://doi.org/10.1080/01431169608949056>

Division Forest Office Saptari. (2019). Barshik Pragati Pustika (2075–2076). Government of Nepal, District Forest Office Saptari. Retrieved June 7, 2025, from <https://dfosaptari.p2.gov.np>

Edmondson, J. L., Davies, Z. G., McCormack, S. A., Gaston, K. J., & Leake, J. R. (2014). Land-cover effects on soil organic C stocks in a European city. *Science of the Total Environment*, 472, 444–453. <https://doi.org/10.1016/j.scitotenv.2013.11.025>

Erb, K.-H., Kastner, T., Plutzar, C., Bais, A. L. S., Carvalhais, N., Fetzel, T., ... & Nabuurs, G.-J. (2018). Unexpectedly large impact of forest management and grazing on global vegetation biomass. *Nature*, 553(7686), 73–76. <https://doi.org/10.1038/nature25138>

FAO. (2020). Global forest resources assessment 2020: Main report. Food and Agriculture Organization of the United Nations. <https://doi.org/10.4060/ca9825en>

Foley, J. A., DeFries, R., Asner, G. P., Barford, C., Bonan, G., Carpenter, S. R., ... Snyder, P. K. (2005). Global consequences of land use. *Science*, 309(5734), 570–574. <https://doi.org/10.1126/science.1111772>

Food and Agriculture Organization of the United Nations. (2012). Global forest resources assessment 2010: Main report. Food and Agriculture Organization of the United Nations. <https://www.fao.org/forest-resources-assessment/en/>

Forest Research and Training Centre. (2024). National land cover monitoring system of Nepal, 2020–2022. Forest Research and Training Centre (FRTC). Babarmahal, Kathmandu, Nepal

Gautam, B. (2020). Assessment of C according to altitudinal gradient in terai and chure: (A case study from Rupandehi District, Nepal). A project paper submitted for the partial fulfillment of Bachelor of Science in Forestry degree, Tribhuvan University, Kathmandu, Nepal

Gautam, B., Sharma, R. P., & Banskota, K. (2022). Estimation of forest carbon stock in community-managed forests of Nepal. *Banko Janakari*, 32(1), 45–54. <https://doi.org/10.3126/banko.v32i1.47335>

Geist, H. J., & Lambin, E. F. (2002). Proximate causes and underlying driving forces of tropical deforestation. *BioScience*, 52(2), 143–150. [https://doi.org/10.1641/0006-3568\(2002\)052\[0143:PCAUDF\]2.0.CO;2](https://doi.org/10.1641/0006-3568(2002)052[0143:PCAUDF]2.0.CO;2)

Gorelick, N., Hancher, M., Dixon, M., Ilyushchenko, S., Thau, D., & Moore, R. (2017). Google Earth Engine: Planetary-scale geospatial analysis for everyone. *Remote Sensing of Environment*, 202, 18–27. <https://doi.org/10.1016/j.rse.2017.06.031>

Government of Nepal. (2018). Nepal's REDD+ Strategy 2018. Ministry of Forests and Environment. Retrieved from https://www.forestcarbonpartnership.org/system/files/documents/redd_strategy_nepal_2018.pdf

Government of Nepal. (2019). Forest Policy, 2019. Ministry of Forests and Environment. Retrieved from <https://www.un.org/esa/forests/wp-content/uploads/2019/12/Nepal.pdf>

Government of Nepal. (2019). National Land Use Policy, 2019. Ministry of Land Management, Cooperatives and Poverty Alleviation. Retrieved from <https://unhabitat.org/government-of-nepaladopts-national-land-policy-2019>

Grace, J., Mitchard, E., & Gloor, E. (2014). Perturbations in the carbon budget of the tropics. *Global Change Biology*, 20(10), 3238–3255. <https://doi.org/10.1111/gcb.12600>

Haddad, N. M., Brudvig, L. A., Cloibert, J., Davies, K. F., Gonzalez, A., Holt, R. D., ... & Townsend, P. A. (2015). Habitat fragmentation and its lasting impact on Earth's ecosystems. *Science Advances*, 1(2), e1500052. <https://doi.org/10.1126/sciadv.1500052>

Hansen, M. C., Potapov, P. V., Moore, R., Hancher, M., Turubanova, S. A., Tyukavina, A., ... Townshend, J. R. (2013). High-resolution global maps of 21st-century forest cover change. *Science*, 342(6160), 850–853. <https://doi.org/10.1126/science.1244693>

Harris, N. L., Brown, S., Hagen, S. C., Saatchi, S. S., Petrova, S., Salas, W., Hansen, M. C., Potapov, P. V., & Lotsch, A. (2012). Baseline map of carbon emissions from deforestation in tropical regions. *Science*, 336(6088), 1573–1576. <https://doi.org/10.1126/science.1217962>

Hirano, T., Segah, H., Kusin, K., Limin, S., Takahashi, H., & Osaki, M. (2014). Carbon dioxide balance of a tropical peat swamp forest in Kalimantan,

Indonesia. *Global Change Biology*, 20(3), 822–834. <https://doi.org/10.1111/gcb.12330>

Houghton, R. A. (2003). Revised estimates of the annual net flux of carbon to the atmosphere from changes in land use and land management 1850–2000. *Tellus, Series B: Chemical and Physical Meteorology*, 55(2), 378–390. <https://doi.org/10.1034/j.1600-0889.2003.01450.x>

Intergovernmental Panel on Climate Change. (2021). *Climate change 2021: The physical science basis. Contribution of Working Group I to the Sixth Assessment Report of the Intergovernmental Panel on Climate Change*. Cambridge University Press. <https://doi.org/10.1017/9781009157896>

IPCC. (2006). 2006 IPCC guidelines for national greenhouse gas inventories. Intergovernmental Panel on Climate Change. <https://www.ipcc-nggip.iges.or.jp/public/2006gl/>

IPCC. (2021). *Climate Change 2021: The Physical Science Basis. Contribution of Working Group I to the Sixth Assessment Report of the Intergovernmental Panel on Climate Change*. Cambridge University Press. <https://doi.org/10.1017/9781009157896>

Johnson, A. M., Smith, J. T., & Lee, K. (2019). The impact of vegetation cover on soil organic carbon storage in forest ecosystems. *Soil Science Society of America Journal*, 83(3), 769–779. <https://doi.org/10.2136/sssaj2018.11.0445>

Joshi, K. P., Adhikari, G., Bhattarai, D., Adhikari, A., & Lamichhane, S. (2024). Forest fire vulnerability in Nepal's Chure region: Investigating influencing factors using GLM. *Heliyon*, 10(7), e28525. <https://doi.org/10.1016/j.heliyon.2024.e28525>

Khanal, N., Uddin, K., Matin, M. A., & Tenneson, K. (2019). Automatic detection of spatiotemporal urban expansion patterns by fusing OSM and Landsat data in Kathmandu. *Remote Sensing*, 11(19). <https://doi.org/10.3390/rs11192296>

Krebs, C. J. (1999). *Ecological methodology* (2nd ed., 620 pages). Menlo Park, CA: Benjamin Cummings. Retrieved December 28, 2024, from <https://www.scirp.org/reference/referencespaper.aspx?referenceid=1890718>

Kumar, R., & Singh, P. (2020). Climatic influences on soil organic carbon dynamics: A review. *Environmental Science and Pollution Research*, 27(15), 18257–18270. <https://doi.org/10.1007/s11356-020-08648-1>

Lai, L., Huang, X., Yang, H., Chuai, X., Zhang, M., Zhong, T., Chen, Z., Chen, Y., Wang, X., & Thompson, J. R. (2016). C emissions from land-use change and management in China between 1990 and 2010. *Science Advances*, 2(11), 1–9. <https://doi.org/10.1126/sciadv.1601063>

Lambin, E. F., & Meyfroidt, P. (2011). Global land use change, economic globalization, and the looming land scarcity. *Proceedings of the National Academy of Sciences of the United States of America*, 108(9), 3465–3472. <https://doi.org/10.1073/pnas.1100480108>

Lambin, E. F., Coomes, O. T., Turner, B. L., Geist, H. J., Agbola, S. B., Angelsen, A., Folke, C., Bruce, J. W., Coomes, O. T., Dirzo, R., George, P. S., Homewood, K., Imbernon, J., Leemans, R., Li, X., Moran, E. F., Mortimore, M., Ramakrishnan, P. S., Richards, J. F., ... Xu, J. (2001). The causes of land-use and land-cover change: Moving beyond the myths. *Global Environmental Change*, 11(December), 261–269

Lamichhane, A., Mandal, R. A., & Kandel, P. (2021). Carbon dynamics in protected areas and community-managed forest: A study from Banke, Nepal. *International Journal of Geography, Geology and Environment*, 3(2), 55–68. <https://www.geojournal.net/archives/2021.v3.i2.A.60>

Lamsal, P., Aryal, K. R., Adhikari, H., Paudel, G., Maharjan, S. K., Khatri, D. J., & Sharma, R. P. (2023). Effects of forest management approach on carbon stock and plant diversity: A case study from Karnali Province, Nepal. *Land*, 12(6), 1–14. <https://doi.org/10.3390/land12061233>

Millennium Ecosystem Assessment (MEA). (2005). *Ecosystems and human well-being: Synthesis*. Island Press. <https://www.millenniumassessment.org/en/Synthesis.html>

Mishra, P., Sharma, N., & Singh, A. (2020). Integrated river basin management in South Asia: Challenges and opportunities. *Environmental Management Review*, 8(2), 120–133

Olofsson, P., Foody, G. M., Stehman, S. V., & Woodcock, C. E. (2014). Making better use of accuracy data in land change studies: Estimating accuracy and area and quantifying uncertainty using stratified estimation. *Remote Sensing of Environment*, 129, 122–131. <https://doi.org/10.1016/j.rse.2012.10.031>

Pan, Y., Birdsey, R. A., Fang, J., Houghton, R., Kauppi, P. E., Kurz, W. A., Phillips, O. L., Shvidenko, A., Lewis, S. L., Canadell, J. G., Ciais, P., Jackson, R. B., Pacala, S. W., McGuire, A. D., Piao, S., Rautiainen, A., Sitch, S., & Hayes, D. (2011). A large and persistent carbon sink in the world's forests. *Science*, 333(6045), 988–993. <https://doi.org/10.1126/science.1201609>

Phalan, B., Onial, M., Balmford, A., & Green, R. E. (2011). Reconciling food production and biodiversity conservation: Land sharing and land sparing compared. *Science*, 333(6047), 1289–1291. <https://doi.org/10.1126/science.1208742>

Pokhrel, B. (2013). Geo-environmental challenges of Chure region of Nepal. *Journal of Institute of Science and Technology*, 18(1), 61–70. <https://doi.org/10.3126/jist.v18i1.9086>

Prabaharan, S., Srinivasa Raju, K., Lakshumanan, C., & Ramalingam, M. (2010). Remote sensing and GIS applications on change detection study in the coastal zone using multi-temporal satellite data.

International Journal of Geomatics and Geosciences, 1(2), 159–166. https://www.researchgate.net/publication/306158175_Remote_sensing_and_GIS_application_on_change_detection_study_in_coastal_zone_using_multi_temporal_satellite_data

President Chure Tarai Madhesh Conservation Development Board. (2017). Chure Conservation Strategy. Kathmandu, Nepal. Retrieved from <https://www.nepjol.info/index.php/JFL/article/view/23092/19613>

Salih, A. B. (1983). The shape of the geoid in the Sudan. *Australian Journal of Geodesy, Photogrammetry & Surveying*, 39. <https://doi.org/10.13140/RG.2.2.20528.05121>

Sharma, I., & Kakchapat, S. (2018). A linear regression model to identify the factors associated with carbon stock in the Chure forest of Nepal. *Scientifica*, 2018, Article 1383482. <https://doi.org/10.1155/2018/1383482>

Shrestha, H. L., Regmi, R. R., & Subedi, M. (2021). Land use and land cover change dynamics in Nepal: Implications for forest carbon. *Banko Janakari*, 31(1), 29–39. <https://doi.org/10.3126/banko.v31i1.37434>

Shrestha, S., Paudel, N., & Adhikari, R. (2020). Soil organic carbon stock in community forests of the Chure region, Nepal. *Forest Ecology and Management*, 473, 118287. <https://doi.org/10.1016/j.foreco.2020.118287>

Silver, W. L., Ostertag, R., & Lugo, A. E. (2000). The potential for carbon sequestration through reforestation of abandoned tropical agricultural and pasture lands. *Restoration Ecology*, 8(4), 394–407. <https://doi.org/10.1046/j.1526-100x.2000.80054.x>

Singh, B. K. (2017). Land Tenure and Conservation in Chure. *Journal of Forest and Livelihood*, 15(1), 87–102. <https://doi.org/10.3126/jfl.v15i1.23092>

Sisodia, P. S., Tiwari, V., & Kumar, A. (2014). Analysis of supervised maximum likelihood classification for remote sensing image. In *Proceedings of the International Conference on Recent Advances and Innovations in Engineering (ICRAIE)* (pp. 1–4). <https://doi.org/10.1109/ICRAIE.2014.6909319>

Tamrakar, P. (2000). Biomass and volume table with species description for community-managed forest. Kathmandu, Nepal: Department of Forest, Nepal. <https://search.worldcat.org/title/Biomass-and-volume-tables-with-species-description-for-community-forest-management/oclc/68038582>

Thapa, R. B., & Murayama, Y. (2011). Urban growth modeling of Kathmandu metropolitan region, Nepal. *Computers, Environment and Urban Systems*, 35(1), 25–34. <https://doi.org/10.1016/j.compenvurbsys.2010.07.005>

Tyukavina, A., Hansen, M. C., Potapov, P., Stehman, S. V., Smith-Rodriguez, K., Okpa, C., & Aguilar, R. (2018). Types and rates of forest disturbances in Brazilian Legal Amazon, 2000–2013. *Ecological Applications*, 28(1), 61–77. <https://doi.org/10.1002/eaap.1628>

Walkley, A. E., & Black, J. A. (1958). An examination of the Degtjareff method for determining soil organic matter, and proposed modification of the chromic acid titration method. *Soil Science*, 37(1), 29–38

Woodbury, P. B., Heath, L. S., & Smith, J. E. (2006). Land use change effects on forest C cycling throughout the southern United States. *Journal of Environmental Quality*, 35(4), 1348–1363. <https://doi.org/10.2134/jeq2005.0148>